Anal. Chem. **2002,** *74,* 4774−4780

Separation and Characterization of Single-Walled and Multiwalled Carbon Nanotubes by Using Flow Field-Flow Fractionation

Bailin Chen and John P. Selegue*

Department of Chemistry and NSF−MRSEC Advanced Carbon Materials Center, University of Kentucky, Lexington, Kentucky 40506-0055

Oxidatively shortened single-walled and multiwalled carbon nanotubes were characterized by using flow field-flow fractionation (FlFFF) under normal and steric modes, respectively. Narrow size fractions were collected from FlFFF separations. The carbon nanotubes in each fraction were further characterized by using scanning and transmission electron microscopy. FlFFF separates carbon nanotubes principally on the basis of length, leading to fractions with relatively uniform lengths. The relationship between nanotube length and FlFFF elution volume is discussed.

Carbon nanotubes show great potential for materials applications. They may be used as nanoprobes, as nanowires, in polymer composites, as electrode components, as catalyst supports,[1−4] and perhaps for hydrogen storage.[5−9] They combine unique electronic structures, high surface area, electrical conductivity, and excellent strength. However, even after 10 years, carbon nanotube applications are slow to enter the marketplace. This is due, at least in part, to the low purity of typical as-produced carbon nanotubes combined with the difficulty of subsequent purification and characterization.

Raw carbon nanotube samples often contain as little as 50% nanotubes, with the rest consisting of impurities such as fullerenes, amorphous carbon, and catalyst residue. In addition, carbon nanotubes frequently form tightly bound bundles, often called "ropes". Pure, monodisperse nanotubes will be essential for specialized applications. Several methods have been introduced to remove some of the impurities from raw nanotubes. Chemical oxidation removes amorphous carbon and catalyst particles at the cost of significant nanotube loss.[10−14] Filtration and centrifugation steps are also used to purify carbon nanotubes,[14−16] but they can introduce new contaminants and cannot provide detailed information about the size of nanotubes. Size exclusion chromatography (SEC) effectively purifies carbon nanotubes.[17−21] Gel permeation chromatography (GPC) can be used to purify single-walled carbon nanotubes, but they must first be shortened to ∼300 nm, polished, and solubilized by attachment of long-chain amines (i.e., single-wall nanotube (SWNT)-$CONH(CH_2)_{17}CH_3$).[22,23] Very recently, we reported the high-resolution separation of SWNTs by using capillary electrophoresis (CE).[24] Unfortunately, SEC, GPC, and CE do not provide direct, detailed information on particle size distributions. In the first report of field-flow fractionation (FFF) of carbon nanotubes, Smalley and co-workers demonstrated that

* To whom correspondence should be addressed. Phone: (859)257-3484. Fax: (859)323-1069. E-mail: selegue@uky.edu.

(1) Tans, S. J.; Devoret, M. H.; Dal, H.; Thess, A.; Smalley, R. E.; Geerligs, L. J.; Dekker: C. *Nature (London)* **1997**, *386*, 474−477.
(2) Yakobson, B. I.; Smalley, R. E. *Am. Sci.* **1997**, *85*, 324.
(3) Sinnott, S. B.; Andrews, R. *Crit. Rev. Solid State Mater. Sci.* **2001**, *26*, 145−249.
(4) Ajayan, P. M. *Chem. Rev.* **1999**, *99*, 1787−1799.
(5) Dillon, A. C.; Jones, K. M.; Bekkedahl, T. A.; Kiang, C. H.; Bethune, D. S.; Heben, M. J. *Nature (London)* **1997**, *386*, 377−379.
(6) Dillon, A. C.; Heben, M. J. *Appl. Phys. A: Mater. Sci. Process.* **2001**, *72*, 133−142.
(7) Hirscher, M.; Becher, M.; Haluska, M.; Dettlaff-Weglikowska, U.; Quintel, A.; Duesberg, G. S.; Choi, Y. M.; Downes, P.; Hulman, M.; Roth, S.; Stepanek, I.; Bernier, P. *Appl. Phys. A: Mater. Sci. Process.* **2001**, *72*, 129−132.
(8) Sumanasekera, G. U.; Adu, C. K. W.; Pradhan, B. K.; Chen, G.; Romero, H. E.; Eklund, P. C. *Phys. Rev. B* **2002**, *65*, 035408/1−035408/5.
(9) Hirscher, M.; Becher, M.; Haluska, M.; Quintel, A.; Skakalova, V.; Choi, Y. M.; Dettlaff-Weglikowska, U.; Roth, S.; Stepanek, I.; Bernier, P.; Leonhardt, A.; Fink, J. *J. Alloys Compd.* **2002**, *330−332*, 654−658.
(10) Saito, R.; Dresselhaus, G.; Dresselhaus, M. S. *Physical properties of carbon nanotubes*; World Scientific Publishing Co.: Singapore, 1998.
(11) Yao, N.; Lordi, V.; Ma, S. X. C.; Dujardin, E.; Krishnan, A.; Treacy, M. M. J.; Ebbesen, T. W. *J. Mater. Res.* **1998**, *13*, 2432−2437.
(12) Liu, J.; Rinzler, A. G.; Dai, H.; Hafner, J. H.; Bradley, R. K.; Boul, P. J.; Lu, A.; Iverson, T.; Shelimov, K.; Huffman, C. B.; Rodriguez-Macias, F.; Shon, Y.-S.; Lee, T. R.; Colbert, D. T.; Smalley, R. E. *Science* **1998**, *280*, 1253−1256.
(13) Vaccarini, L.; Goze, C.; Aznar, R.; Micholet, V.; Journet, C.; Bernier, P. *Synth. Met.* **1999**, *103*, 2492−2493.
(14) Holzinger, M.; Hirsch, A.; Bernier, P.; Duesberg, G. S.; Burghard, M. *Appl. Phys. A: Mater. Sci. Process.* **2000**, *70*, 599−602.
(15) Bandow, S.; Asaka, S.; Zhao, X.; Ando, Y. *Appl. Phys. A: Mater. Sci. Process.* **1998**, *A67*, 23−27.
(16) Shelimov, K. B.; Esenaliev, R. O.; Rinzler, A. G.; Huffman, C. B.; Smalley, R. E. *Chem. Phys. Lett.* **1998**, *282*, 429−434.
(17) Duesberg, G. S.; Muster, J.; Krstic, V.; Burghard, M.; Roth, S. *Appl. Phys. A: Mater. Sci. Process.* **1998**, *A67*, 117−119.
(18) Duesberg, G. S.; Burghard, M.; Muster, J.; Philipp, G.; Roth, S. *Chem. Commun.* **1998**, 435−436.
(19) Duesberg, G. S.; Muster, J.; Byrne, H. J.; Roth, S.; Burghard, M. *Appl. Phys. A: Mater. Sci. Process.* **1999**, *69*, 269−274.
(20) Duesberg, G. S.; Blau, W. J.; Byrne, H. J.; Muster, J.; Burghard, M.; Roth, S. *Chem. Phys. Lett.* **1999**, *310*, 8−14.
(21) Duesberg, G. S.; Blau, W.; Byrne, H. J.; Muster, J.; Burghard, M.; Roth, S. *Synth. Met.* **1999**, *103*, 2484−2485.
(22) Niyogi, S.; Hu, H.; Hamon, M. A.; Bhowmik, P.; Zhao, B.; Rozenzhak, S. M.; Chen, J.; Itkis, M. E.; Meier, M. S.; Haddon, R. C. *J. Am. Chem. Soc.* **2001**, *123*, 733−734.
(23) Zhao, B.; Hu, H.; Niyogi, S.; Itkis, M. E.; Hamon, M. A.; Bhowmik, P.; Meier, M. S.; Haddon, R. C. *J. Am. Chem. Soc.* **2001**, *123*, 11673−11677.
(24) Doorn, S. K.; Fields, R. E., III; Hu, H.; Hamon, M. A.; Haddon, R. C.; Selegue, J. P.; Majidi, V. *J. Am. Chem. Soc.* **2002**, *124*, 3169−3174.

10.1021/ac020111b CCC: $22.00
Published on Web 08/07/2002

the technique separated oxidatively shortened SWNTs on the basis of length. In this study, FFF-separated SWNTs were electrodeposited on highly oriented pyrolytic graphite (HOPG) surfaces and their lengths measured by atomic force microscopy (AFM).[12] Kim et al. also reported a brief FFF study of the length distribution of SWNTs before and after acid shortening but relied on spherical standards for size estimate.[25] No detailed study of the FFF separation of SWNTs, and no FFF separations of multiwalled carbon nanotubes (MWNTs) at all, have been reported.

FFF is a chromatography-like separation and sizing technique based on elution through a thin, empty channel. The main difference between FFF and chromatography is that FFF separation is (ideally) induced only by physical interactions with an external field rather than physicochemical interactions with a stationary phase.[26−30] FFF is based on the application of a field perpendicular to the fluid flow down the axis of a thin channel (100−500 μm). This externally applied field drives unlike particles to different average positions across the thin channel, where they are caught up at different flow velocities and are thus eluted at different times. The most common fields are cross-flow of a carrier liquid and centrifugation, giving rise to flow FFF (FlFFF) and sedimentation FFF (SedFFF) subtechniques.[31,32] Other perpendicular fields include thermal, electrical, and magnetic fields.[26−30]

For a small particle, typically less than 1 μm, elution time depends on the diffusivity of a particle and its interaction with the field. Separations in this mode, termed normal mode, result in smaller particles eluting ahead of larger particles. Larger particles tend to stay near the channel wall and move through the channel with lower flow velocities. An alternative mode, termed steric or hyperlayer mode, is designed for sizing particles larger than 1 μm.[33] A reversal of the elution order is achieved because the larger particles necessarily protrude into regions of higher flow velocity. Utilizing these two modes, it is possible to probe a mass range spanning 15 orders of magnitude, from molecules of 1000 Da molecular mass up to particles 100 μm in diameter.[27] FFF is uniquely capable of separating materials over such a wide size range.

Since carbon nanotubes often have a broad size distribution, it is easy to appreciate that FFF with its wide and flexible range of operating parameters is an ideal tool to divide these broad distributions into discrete, roughly monodisperse fractions for further characterization. FlFFF was used in this work because of the above advantages as well as its high resolution. Although FlFFF is primarily an analytical-scale technique, there has been some success in developing synthetic-scale SPLITT separations based on FFF results.[34−36]

The theory of FFF has been detailed elsewhere.[30,37−39] Applications in industry, biomedicine, and environmental science have been widely developed.[40−44] FlFFF theory is almost entirely based on the assumption of spherical particles, with a few pioneering exceptions.[45,46] Conventional FFF theory is not applicable to cylindrical, hollow carbon nanotubes. Nonetheless, we are empirically searching for suitable FFF separation conditions that will enable the routine separation of carbon nanotubes on the basis of their diameters or lengths. We report here our initial results with oxidatively shortened SWNTs and MWNTs.

EXPERIMENTAL SECTION

Samples. The single-walled carbon nanotubes used in this study were prepared by using a modified electric arc method.[47] The raw nanotubes were purified and shortened by using nitric acid oxidation, followed by centrifugation, resuspension, and cross-flow filtration steps.[12,48,49] The process removed most of the amorphous carbon, but treated samples still contained significant amounts of catalyst particles and graphite particles as confirmed by transmission electron microscopy (TEM).

The raw multiwalled carbon nanotubes were prepared by using a chemical vapor deposition (CVD) method.[50] The raw MWNTs were oxidized with a mixture of 0.5 M $KMnO_4$ and 0.5 M H_2SO_4 at 150 °C for 5 h, followed by filtration through a 0.2-μm filter membrane to remove nanoparticles. The residual solid was air-dried at room temperature prior to FlFFF. The product obtained in this way contained over 95% MWNTs as confirmed by electron microscopy.

Carrier Liquid and Standards. The carrier liquid was pure, deionized Milli-Q water (Millipore) containing 0.05% (w/v) sodium dodecyl sulfate (SDS), a surfactant to aid in suspension of the nanotubes, and 0.02% (w/v) sodium azide, a bactericide. The water was filtered through a 0.2-μm membrane before use, and the carrier fluid was passed through Millipore 10-μm HPLC inlet solvent filters in the channel and cross-flow delivery lines. To

(25) Kim, H. Y.; Choi, W. B.; Lee, N. S.; Chung, D. S.; Kang, J. H.; Han, I. T.; Kim, J. M.; Moon, M. H.; Kim, J. S. *Mater. Res. Soc. Symp. Proc.* **2000**, *593*, 123−127.
(26) Janca, J. *J. Chromatogr. Libr.* **1992**, *51A*, A449−A479.
(27) Giddings, J. C. *Science* **1993**, *260*, 1456−1465.
(28) Giddings, J. C.; Williams, P. S. *Am. Lab. (Shelton, Conn.)* **1993**, *25*, 88, 90−85.
(29) Janca, J. *Mikrochim. Acta* **1993**, *111*, 135−162.
(30) Schimpf, M. E., Caldwell, K., Giddings, J. C., Eds. *Field-flow fractionation handbook*; Wiley-Interscience: New York, 2000.
(31) Giddings, J. C.; Yang, F. J. F.; Myers, M. N. *Anal. Chem.* **1974**, *46*, 1917−1924.
(32) Giddings, J. C. *Anal. Chem.* **1981**, *53*, 1170A−1172A, 1174A, 1176A, 1178A.
(33) Moon, M. H. In *Field-flow fractionation handbook*; Schimpf, M. E., Caldwell, K., Giddings, J. C., Eds.; Wiley-Interscience: New York, 2000; pp 383−396.
(34) Giddings, J. C. *Anal. Chem.* **1985**, *57*, 945−947.
(35) Fuh, C. B.; Giddings, J. C. *J. Microcolumn Sep.* **1997**, *9*, 205−211.
(36) Gao, Y.; Myers, M. N.; Barman, B. N.; Giddings, J. C. *Part. Sci. Technol.* **1991**, *9*, 105−118.
(37) Giddings, J. C.; Myers, M. N.; Caldwell, K. D.; Fisher, S. R. *Methods Biochem. Anal.* **1980**, *26*, 79−136.
(38) Giddings, J. C. *Sep. Sci. Technol.* **1984**, *19*, 831−847.
(39) Janca, J. *Chromatogr. Sci.* **1988**, *39*, 336 pp.
(40) Giddings, J. C.; Chen, X.; Wahlund, K. G.; Myers, M. N. *Anal. Chem.* **1987**, *59*, 1957−1962.
(41) Beckett, R.; Jue, Z.; Giddings, J. C. *Environ. Sci. Technol.* **1987**, *21*, 289−295.
(42) Beckett, R.; Hart, B. T. In *Environmental Particles*; Buffle, J., van Leeuwen, H. P., Eds.; Lewis Publishers: Boca Raton, FL, 1993; Vol. 2, pp 165−205.
(43) Chen, B.; Shand, C. A.; Beckett, R. *J. Environ. Monit.* **2001**, *3*, 7−14.
(44) Chen, B.; Beckett, R. *Analyst (Cambridge, U. K.)* **2001**, *126*, 1588−1593.
(45) Beckett, R.; Jiang, Y.; Liu, G.; Moon, M. H.; Giddings, J. C. *Part. Sci. Technol.* **1994**, *12*, 89−113.
(46) Kirkland, J. J.; Schallinger, L. E.; Yau, W. W. *Anal. Chem.* **1985**, *57*, 2271−2275.
(47) Journet, C.; Maser, W. K.; Bernier, P.; Loiseau, A.; Lamy de la Chapells, M.; Lefrant, S.; Deniard, P.; Lee, R.; Fischer, J. E. *Nature (London)* **1997**, *388*, 756−758.
(48) Rinzler, A. G.; Liu, J.; Dai, H.; Nikolaev, P.; Huffman, C. B.; Rodriguez-Macias, F. J.; Boul, P. J.; Lu, A. H.; Heymann, D.; Colbert, D. T.; Lee, R. S.; Fischer, J. E.; Rao, A. M.; Eklund, P. C.; Smalley, R. E. *Appl. Phys. A: Mater. Sci. Process.* **1998**, *A67*, 29−37.
(49) Chen, Y.; Haddon, R. C.; Fang, S.; Rao, A. M.; Eklund, P. C.; Lee, W. H.; Dickey, E. C.; Grulke, E. A.; Pendergrass, J. C.; Chavan, A.; Haley, B. E.; Smalley, R. E. *J. Mater. Res.* **1998**, *13*, 2423−2431.
(50) Andrews, R.; Jacques, D.; Rao, A. M.; Derbyshire, F.; Qian, D.; Fan, X.; Dickey, E. C.; Chen, J. *Chem. Phys. Lett.* **1999**, *303*, 467−474.

monitor the performance of the FlFFF instrument and to calibrate the size distribution of nanotubes, polymer standard beads of 0.050, 0.100, 0.150, 5, and 10 μm (Duke Scientific, Palo Alto, CA) were used as standard materials, with one drop of the concentrated suspension dispersed in 5 mL of FlFFF carrier solution.

Sample Preparation for FlFFF. The single-walled or multi-walled nanotubes (5.0 mg), treated as described above, were weighed into a 25-mL glass vial. FlFFF carrier solution (15 mL) was added, and the mixture was dispersed and homogenized by sonicating for 3 min with a 650-W sonic horn (Sonics and Materials Inc., Danbury, CT, model VCX-600) at 50% duty cycle and an output level of four while cooling with ice. The sample suspension was resonicated for 30 s to disperse any aggregates immediately prior to being injected into the FlFFF channel.

MWNTs were preseparated by using centrifugation. The shortened MWNTs were isolated by repeated centrifugation at 2450 rpm for 30 min in a Clay-Adams Dynac centrifuge, followed by resuspension; the procedure was repeated at least five times. The supernatant, containing ~10% of the original material, was discarded. The solid material was resuspended in FlFFF carrier solution at a concentration of ~0.1 mg·mL^{-1} prior to injection.

Sonication Time. Experiments to test the influence of different sonication times on samples were performed on the MWNT sample. The sample preparation and preseparation procedures were the same as described above, except that sonication times of 1, 2, 5, 10, 20, and 60 min were applied before FlFFF analysis.

Sample Preparation for Scanning Electron Microscpy (SEM). Initial attempts to use an electrochemical deposition method similar to that of Liu et al.[12] to deposit SWNTs and MWNTs for SEM gave unsatisfactory results. The samples were so heavily contaminated with surfactant and other impurities that it was not possible to discern features of the nanotubes themselves. We devised a simple filtration method to prepare FlFFF fractions for SEM.

A 2-mm hole was cut out of the center a ~5-cm length of Scotch Magic Tape. A piece of an alumina filter membrane (Whatman Anodisc 13, pore size 0.020 μm) was attached to the tape, fully covering the 2-mm hole. The tape with the filter membrane was placed on a glass vacuum filter holder. A small volume (~0.3 mL) of a FlFFF fraction (or a diluted sample of the original sample suspension) was suction-filtered through the membrane, followed by washing with a few drops of Milli-Q water to remove the surfactant. After filtration, the membrane was dried at room temperature, cut from the tape, and placed onto the copper plate of the SEM specimen holder. The sample was finally coated with Au (Emscope, model SC 400) prior to SEM measurement.

FlFFF, SEM, and TEM Instrumentation. FlFFF was conducted by using a FFFractionation LLC Universal Fractionator model F1000. The channel was 29.4 cm long, 0.0190 cm thick, and 2.0 cm wide. The geometrical void volume was 1.05 cm^3. A regenerated cellulose membrane with a 20 000-Da molecular mass cutoff was used. Samples (20 μL containing ~2 μg of nanotubes) were injected into the channel through a Rheodyne sample injection port. Two Intelligent Pump model 301 HPLC pumps were used to deliver carrier liquid in the channel and nonrecirculating cross-flows. Fractograms were obtained by monitoring the absorbance of the eluent at 254 nm with a Linear Instrument model 200UV/Visible detector. For the SWNT sample, a channel flow of 0.3 mL·min^{-1}, a cross-flow of 0.5 mL·min^{-1}, and an equilibrium time of 10 min were used. During the equilibrium time, the cross-flow establishes a steady-state distribution of the particles in the channel prior to initiation of the channel flow. For the MWNT sample, a cross-flow of 0.3 mL·min^{-1} was applied during a 7-min equilibrium time. After equilibrium was established, elution was carried out at a channel flow of 0.3 mL·min^{-1} and a cross-flow rate of 0.03 mL·min^{-1}, decreased by restricting the outlet of the cross-flow line with a flow regulator that was calibrated prior to the FlFFF run.

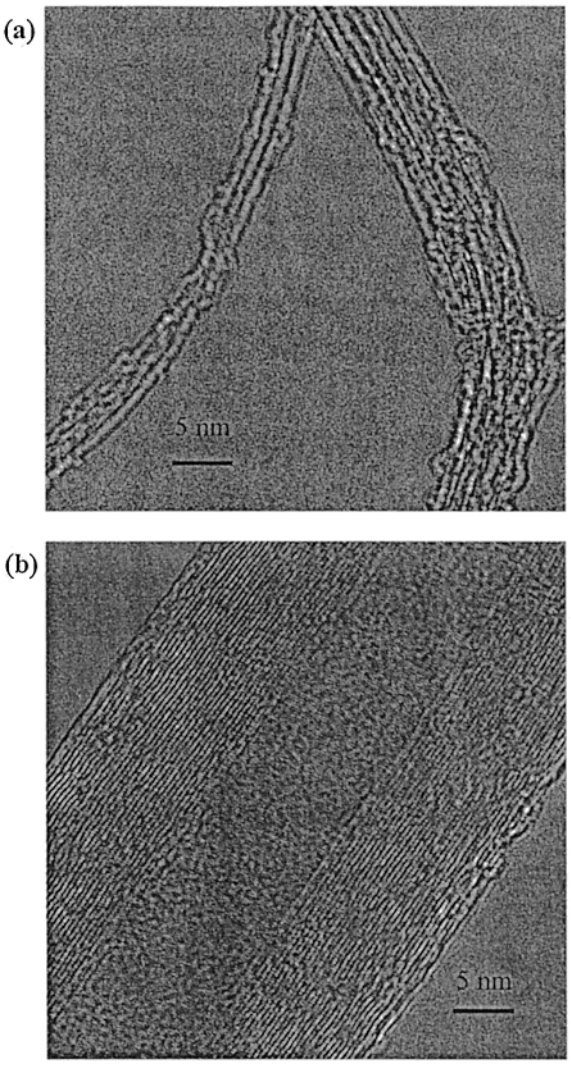

Figure 1. High-resolution transmission electron microscopy images of (a) SWNTs and (b) MWNTs.

Microscopy of the FlFFF fractions was measured by using a Hitachi S900 field-emission scanning electron microscope with ultrahigh resolution or a high-resolution JEOL 2010F field-emission transmission electron microscope.

RESULTS AND DISCUSSION

Sample Confirmation. SWNTs and MWNTs were examined by high-resolution TEM prior to FlFFF separation. Typical micrographs are shown in Figure 1. It is evident from Figure 1a that the SWNT sample consists largely of bundles of tubes with individual diameters of ~1.2 nm. In contrast, nearly no bundles are found in the MWNT sample. Typical spacings of ~0.36 nm

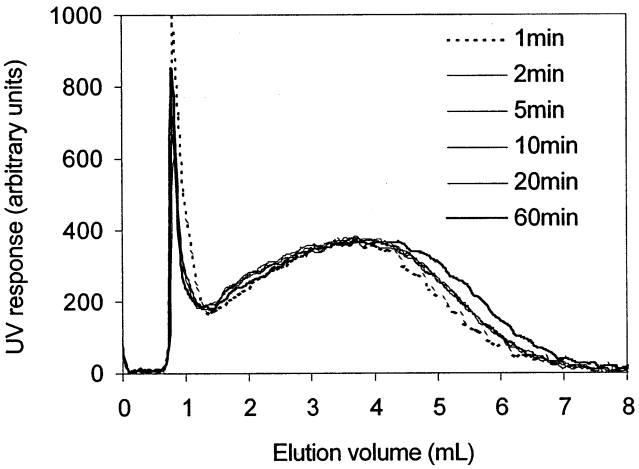

Figure 2. FlFFF fractograms of MWNTs with various sonication times.

between the graphitic layers as well as the hollow channel in the middle of the MWNTs are seen in Figure 1b.

Sample Sonication Time. A stable, homogeneous suspension is necessary for FlFFF separation. In general, this can be achieved by dispersing carbon nanotubes in water with the assistance of a surfactant and sonication. Previous investigators[17,25,51] reported sonication times from 2 min to a few hours. At short sonication times, the carbon nanotubes may not be dispersed well; at long sonication times, the nanotubes may be damaged.

Figure 2 shows the FlFFF fractograms of MWNTs with different sonication times. Following the initial void peak in the UV fractogram (very fine and dissolved material that is not retained under the conditions of the experiment), the MWNTs elute as a broad peak. A sonication time of 1 min leads to less long-elution-time material and an overall weaker fractogram, indicating that a sonication time of 1 min is too short for 15 mL of suspension. In contrast, the UV response using a sonication time of 60 min was slightly shifted to later elution times, illustrating that some carbon nanotubes are "clipped" by long sonication (shorter tubes are eluted later in this steric mode separation; vide infra in MWNT Fractionation). A 2-min sonication time seems to be optimal for initial sonication of 15 mL of suspension. Longer sonication time does not improve the dispersion. The sample was resonicated for 30 s immediately before each FFF injection to ensure a uniform suspension.

SWNT Fractionation. A typical FlFFF fractogram of SWNTs, SEM micrographs from measuring SWNT samples both before FlFFF separation, and the fractions collected at certain elution volume during FlFFF separation are shown in Figure 3. Vertical bars on the fractogram mark the collection volumes of the fractions. The fractograms of standard materials with 0.050- and 0.100-μm spherical diameters are also plotted in Figure 3.

The SEM images in Figure 3 illustrate that SWNTs can be successfully fractionated using Fl/normal FFF. Well-populated areas were chosen for Figures 3 and 5; the amount of material appearing in the SEM images is not necessarily proportional to the UV detector response for the specified fractions. Some nanoparticles were also observed in SEM images of the SWNTs

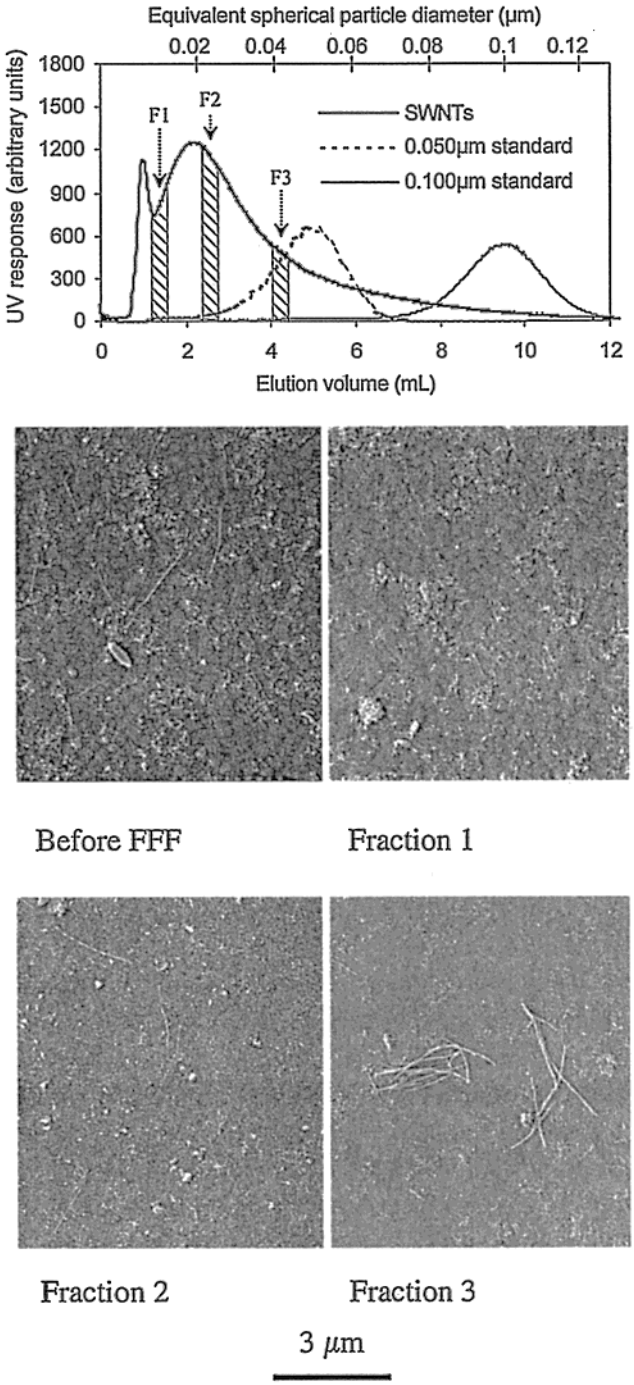

Figure 3. (Top) FlFFF fractograms of SWNTs and standards. (Bottom) SEM images of SWNTs before and after FlFFF separation. The SEM images were measured at a magnification of 10 K.

before and after FlFFF separation, indicating that treatment with nitric acid did not to remove all impurities in the nanotubes. TEM images (not presented here) also confirmed the presence of nanoparticle impurities in FlFFF fractions of SWNTs.

The top scale of Figure 3 shows the equivalent spherical particle diameter calculated from the fractogram of the SWNTs based on Fl/normal FFF theory. The results show that the distribution of SWNTs is equivalent to a distribution of spherical particles with diameters ranging from 0.007 to 0.12 μm. This size range is within the range of normal-mode FlFFF separation. The SEM images obtained from the FlFFF fractions in Figure 3

(51) Abatemarco, T.; Stickel, J.; Belfort, J.; Frank, B. P.; Ajayan, P. M.; Belfort, G. *J. Phys. Chem. B* **1999**, *103*, 3534−3538.

Table 1. Dimensions and Retention Volumes of FlFFF-Fractionated SWNTs and MWNTs

sample	fraction no.	mean NT length (μm)[a]	mean NT diam (μm)[a]	aspect ratio	NT vol (μm^{-3})	retention vol (mL)[b]
SWNTs (including bundles)	1	0.63(4)	0.008(1)	79	0.000032	1.35
	2	1.1(3)	0.023(4)	48	0.00046	2.55
	3	1.9(3)	0.056(5)	34	0.0047	4.20
MWNTs	1	20(2)	0.16(3)	122	0.39	1.42
	2	10(2)	0.15(3)	67	0.18	4.12
	3	4.8(8)	0.13(2)	37	0.064	6.22

[a] Mean NT lengths and diameters were calculated by measuring at least 30 nanotubes on several SEM images of the same sample. The usual equation was used to calculate the confidence limits for a 95% confidence level.[60] The number in parentheses indicates the confidence limits of the last digit of the value. [b] The precision of retention volumes is ~0.01 mL.

demonstrate that the lengths and diameters of the SWNTs increase with increasing elution volume.

The length of a nanotube is much greater than the diameter of a spherical particle with the same FlFFF elution time under identical conditions; i.e., a nanotube of a certain length is eluted well ahead of a sphere with that diameter. Since the retention time (or volume) of a particle depends on the particle's diffusivity and the field strength, and since the mass of a certain length tube is much less than that of a sphere of that diameter, the tube with a larger diffusivity reaches an equilibrium position farther away from the accumulation wall than does the sphere, resulting in earlier elution of the tube. Further, the flexibility of SWNTs probably allows them to wrap into a shape smaller than their sphere of rotation.

The length and diameter of single or bundled SWNTs were determined for each fraction by using SEM and TEM. Prior to separation, the lengths of the SWNTs and bundles ranged from 0.3 to 4.5 μm. After separation, SWNTs length ranges were 0.4−0.8 μm in fraction 1, 1.0−2.6 μm in fraction 2, and 1.5−3.9 μm in fraction 3. The mean lengths, diameters, aspect ratios, and volumes of SWNTs, together with the corresponding retention volumes, are summarized in Table 1. Virtually all SWNTs are found in bundles with aspect ratios between 34 and 79, with the bundles of highest aspect ratio in fraction 1. Single SWNTs have diameters in the range of 1.2−1.4 nm, with lengths in the micrometer range and a pronounced tendency to agglomerate into bundles.[52] Although we cannot rule out bundle formation after elution, most likely the SWNTs eluted through the FFF channel as the bundles observed by SEM of the sample prior to FlFFF separation. In the SEM image of fraction 3, hardly any unbundled tubes are seen. Because of the increased tendency of nanotubes to form bundles in concentrated suspensions, the most dilute suspension that maintains an adequate detector response will give the best separation.

The data in Table 1 also show that nanotubes are eluted ahead of spherical particles with the same volume. Aside from the difference in shape, the hollow structure and resulting low density of nanotubes may cause them to move farther from the accumulation wall compared to spheres, resulting in faster elution of the nanotubes. Although diffusion plays a dominant role in determining elution time in a normal mode separation, complicated motions such as tumbling and rolling may also affect the elution of nanotubes.

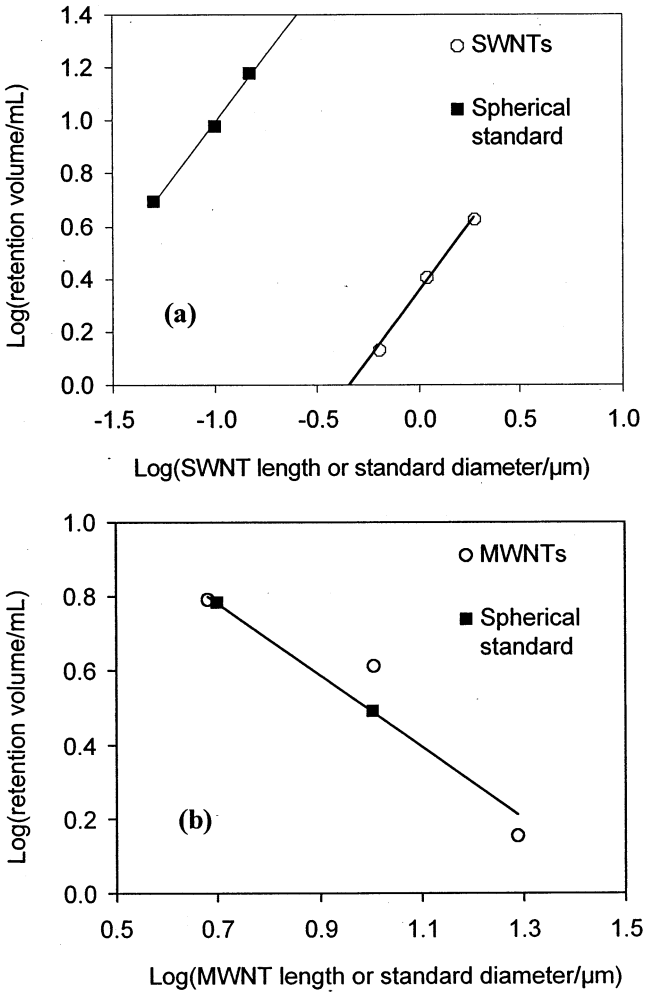

Figure 4. Logarithm of the elution volume V_r versus the logarithm of the diameter of spherical standards and the length of carbon nanotubes for (a) SWNTs and (b) MWNTs.

One can establish an empirical relationship between the retention volume V_r and the length l of nanotubes. Figure 4a shows a plot of $\log(V_r)$ versus $\log(l)$ for SWNTs, based on the average length and elution volume of the nanotube fractions in Figure 3. Such a plot is normally a nearly straight line for a normal-mode separation.[45,53] Figure 4a shows a slight deviation from linearity, possibly due to concomitant increase in SWNT diameter with increasing SWNT length. Length-based selectivity, which reflects

(52) Ebbesen, T. W. *Acc. Chem. Res.* **1998**, *31*, 558−566.

(53) Giddings, J. C.; Moon, M. H.; Williams, P. S.; Myers, M. N. *Anal. Chem.* **1991**, *63*, 1366−1372.

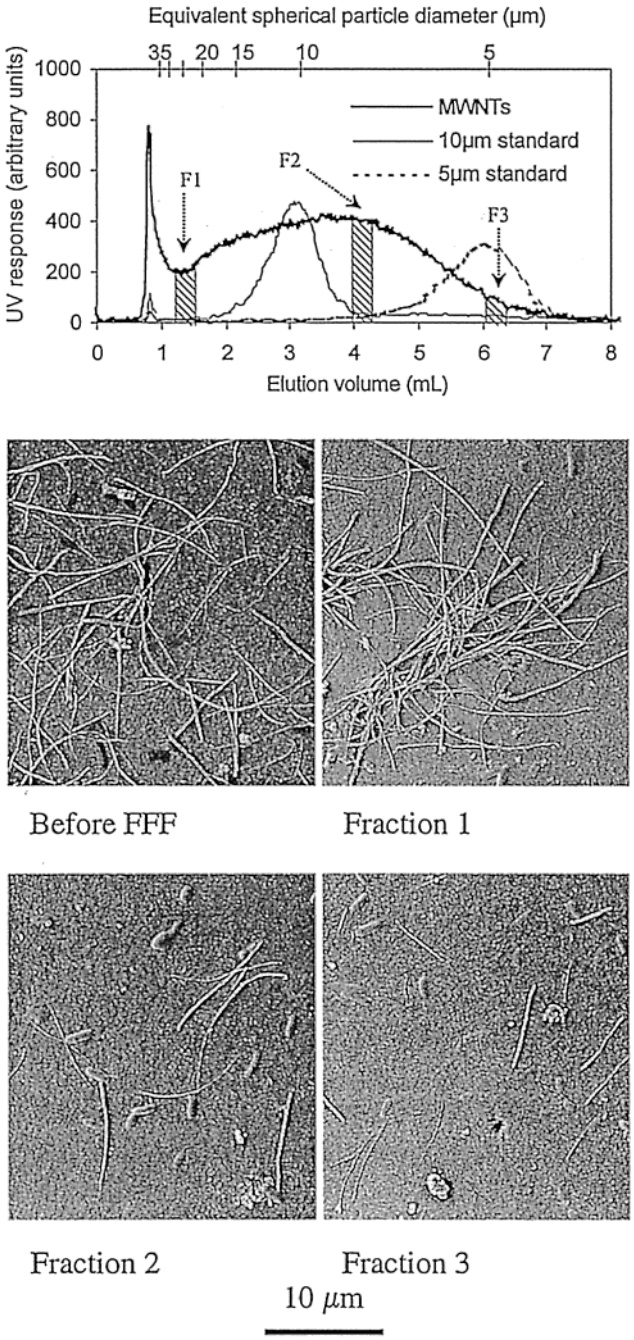

Figure 5. (Top) FlFFF fractograms of MWNTs and standards. (Bottom) SEM images of MWNTs before and after FlFFF separation. The SEM images were measured at a magnification of 3 K.

the separation effectiveness, is calculated as the absolute value of d log(V_r) divided by the absolute value of d log(l).[45] The selectivity is ~1.0 for SWNTs compared to $S_d \approx 0.6-0.8$ for spherical particles and shows that good resolution can be achieved for the separation of SWNTs. That the selectivity value for SWNTs is greater than that of spheres probably reflects the fact that the SWNTs in this study were shortened by treatment with oxidizing acids prior to separation.

MWNT Fractionation. The fractograms obtained for the MWNTs along with standard spherical particles 5 and 10 μm in diameter are plotted in Figure 5. The SEM micrographs of the MWNTs before FlFFF separation and the fractions collected at certain elution volumes during the FFF run are also presented. Vertical bars in the figure indicate the collection volume ranges of the fractions. The SEM images show that the retention volume increases with decreasing nanotube length. This elution order is opposite that of the SWNTs, indicating that MWNTs elute from the channel in *steric* rather than normal mode. Prior to separation, the lengths of the MWNTs ranged from 3 to 33 μm. After separation, MWNTs length ranges were 15−28 μm in fraction 1, 6−17 μm in fraction 2, and 3−10 μm in fraction 3. The mean lengths, diameters, aspect ratios, and volumes of MWNTs, together with the corresponding retention volumes, are summarized in Table 1.

In general, high flow rates are employed in steric mode separations because increasing flow rate increases lift forces, resulting in good separation. However, no satisfactory FFF fractogram of the samples was obtained with flow rates higher than 0.5 mL·min^{-1}. Possibly nanotubes become entangled in the regenerated cellulose membrane under the relatively high channel pressures resulting from high flow rates, rather than being lifted away from the membrane as in the usual steric-mode experiment. In support of this idea, recirculating cross-flow, which also builds up high pressure in the FlFFF channel, resulted in very poor MWNT separations.

Unlike the separation of SWNTs under normal elution mode, the equivalent spherical particle size distribution cannot be directly calculated for the separation of MWNTs conducted under steric elution mode. This is because, in steric mode, there are lift forces, "slip" forces, and particle−wall interactions. As these forces are usually not known accurately, it is impossible to extract size information from first principles. In general, to calibrate and obtain the size distribution of the sample, at least two standard materials must be measured under the same conditions as the sample. The equivalent spherical particle diameter of the sample is shown on the horizontal axis on the top of the figure. The diameter was calculated from the fractograms of two standard materials (5 and 10 μm), based on the linear relationship between log(V_r) and log(diameter). The results indicate that the distribution of MWNTs was equivalent to a distribution of spherical particles with diameters from 3 to 35 μm.

Preliminary experiments were conducted using acid-treated MWNTs dispersed in the FlFFF carrier solution without any preseparation. However, despite the good appearance of the fractograms, SEM of eluted fractions showed poor uniformity in MWNT length. In particular, some very short nanotubes were coeluted with long tubes. This problem arises because the length distribution of the MWNTs spans the range of both normal (<1 μm) and steric (> 1 μm) elution modes. We devised a preseparation step[54] to remove the short MWNTs. MWNTs with behavior equivalent spheres smaller than 1 μm were removed by at least five cycles of centrifugation at 2450 rpm (assuming a MWNTs density of ~1.5 g·cm^{-3}),[55] followed by resuspension in FlFFF carrier solution. This rough preseparation left the shorter nanotubes and other particles that separate in normal mode, ~10% of the total, in the supernatant, which was discarded. The longer MWNTs in the precipitate were resuspended in FlFFF carrier solution for separation in steric mode.

(54) Myers, M. N.; Giddings, J. C. *Anal. Chem.* **1982**, *54*, 2284−2289.
(55) Allen, T. *Particle Size Measurement, Volume 1: Powder Sampling and Particle Size Measurement*; Chapman & Hall: London, 1997.

Relatively uniform MWNTs were found in each SEM image of the fractions in Figure 5, indicating that a good preseparation was achieved. This finding also demonstrated that Fl/steric FFF could successfully fractionate the MWNTs with lengths from 3 to 35 μm. MWNTs give much better SEM images than SWNTs because of the larger MWNT diameters (∼10−280 nm) compared to SWNTs (∼1.2 nm, bundles ∼4−83 nm). TEM micrographs of the FlFFF fractions (not shown here) showed typical MWNT interlayer spacings.

Figure 5 shows that a MWNT is eluted later than a spherical particle with diameter equal to the MWNT's length. This was anticipated because, in steric mode, the diffusion rates of rather large equivalent spheres are negligible. Since the surface of the tubes is much smaller than that of spheres, the tubes present a much smaller cross section to the streamflow than did the spheres. Hence, the tubes were transported more slowly by the channel flow and eluted later than the spheres.

The average length, diameter, volume, and aspect ratio of the MWNTs are summarized in Table 1. The aspect ratios of these MWNTs, ranging from 37 to 122, were even higher than those of the SWNTs. The aspect ratio of the MWNTs increases with their length. We observed no MWNT bundles by SEM. Despite the lack of bundling, dilute suspensions of MWNTs, like SWNTs, show better FlFFF separation.

Table 1 also shows that MWNTs are eluted before spherical particles of the same volume. This behavior is consistent with that observed for the SWNTs and with the results of Beckett et al.[45] on other nonspherical particles. The present results suggest that nanotubes migrate mainly in a tumbling, as opposed to rolling, motion in the FFF channel. It is possible that the elution behavior of nanotubes resembles the alignment of DNA in a flow stream, sometimes called the biased reptation model, observed by Yeung[56,57] and others.[58,59] Doorn et al. observed similar alignment of shortened SWNTs along the axis of elution in capillary electrophoresis separatins.[24]

Figure 4b is a plot of log(V_r) versus log(l) for the MWNTs. Unlike the SWNTs, the log(V_r)−log(l) plot for the MWNTs was nonlinear. The length-based selectivity of the MWNTs increased with increasing nanotube length, again consistent with the results of Beckett et al.[45] The selectivity is ∼0.55 for an average nanotube length 4.8 μm, increasing to 1.61 for a nanotube length of 19.5 μm. The typical value of selectivity for spherical particles in Fl/steric FFF is 1.1−1.5. The increasing selectivity with length of MWNTs is probably due to their greater length, higher aspect ratio, and more rigid structures, compared to SWNTs. Future work is aimed toward a more quantitative relationship between retention volume and the nanotube length.

CONCLUSIONS

Oxidatively shortened single-walled and multiwalled carbon nanotubes with high aspect ratios in the range of 79 and 122, respectively, can be fractionated by using FlFFF in normal mode for SWNTs or steric mode for MWNTs. Stable, homogeneous, representative suspensions of carbon nanotubes can be achieved with minimal sample damage by optimizing the sonication time. SEM images of fractionated nanotubes show that the relationship between the logarithm of the retention volume V_r and the logarithm of the carbon nanotube length l is roughly linear for smaller, more flexible SWNTs but nonlinear for longer, more rigid MWNTs. For MWNTs, retention volume apparently depends on a combination of the length, diameter, and rigidity. The length-based selectivity of MWNTs increases with the length of the nanotubes. More work is required to establish a quantitative relationship.

Field-flow fractionation may prove to be the method of choice for the analysis of nanotube reactions. It provides a quick way to look at the effects of sonication or chemical treatment by following changes in particle size distribution. Although FFF separations are not easily scaled up, relatively uniform length carbon nanotube samples can be obtained by collecting narrow FlFFF fractions. The fractions are suitable for further characterization by using scanning and transmission electron microscopy, as well as spectroscopic probes such as Raman spectroscopy.

ACKNOWLEDGMENT

We are grateful to the U.S. Department of Energy (DE-FG02-00ER45847 and subcontract 10186-00-23) and the MRSEC Program of the National Science Foundation (DMR-9809686) for support. We thank Mark S. Meier, Zhongwen Wang, and Rodney Andrews (University of Kentucky and the Center for Applied Energy Research) and Robert C. Haddon and Mark Hamon (University of California, Riverside) for providing the nanotube samples, Ronald Beckett (Monash University) for valuable discussions, Apparao M. Rao (Clemson University) for Raman spectra, and Alan Dozier, Larry Rice, Dali Qian, and Liming Yuan (University of Kentucky) for help with electron microscopy.

Received for review February 19, 2002. Accepted July 8, 2002.

AC020111B

(56) Kim, Y.; Yeung, E. S. *J. Chromatogr., A* **1997**, *781*, 315−325.
(57) McGregor, D. A.; Yeung, E. S. *J. Chromatogr.* **1993**, *652*, 67−73.
(58) Slater, G. W.; Desruisseaux, C.; Hubert, S. J. In *Capillary electrophosesis of nucleic acids*; Mitchelson, K. R., Cheng, J., Eds.; Methods in Molecular Biology 162; Humana Press: Totowa, NJ, 2001; pp 27−41.
(59) Quesada, M. A.; Menchen, S. In *Capillary electrophosesis of nucleic acids*; Mitchelson, K. R., Cheng, J., Eds.; Methods in Molecular Biology 162; Humana Press: Totowa, NJ, 2001; pp 139−166.
(60) Skoog, D. A.; West, D. M.; Holler, F. J. In *Analytical Chemistry*, 6th ed.; Saunders College Publishing: Philadelphia, PA, 1994; pp 78−95.